The 5-methyl-deoxy-cytidine localization to reveal *in situ* the dynamics of DNA methylation chromatin pattern in a variety of plant organ and tissue cells during development

Pilar S. Testillano*, María-Teresa Solís, María C. Risueño

Plant Development and Nuclear Architecture, Biological Research Centre, CIB-CSIC

Ramiro de Maeztu 9, 28040 Madrid, Spain

*Corresponding author

E-mail: testillano@cib.csic.es

Phone: +3418373112

Fax: +3415360432

Running title: Approach for *in situ* DNA methylation pattern during plant development

Key words: Epigenetics, plant cell nucleus, proliferation, differentiation, quiescent cell, cycling cell, chromosomes, confocal microscopy.

ABSTRACT

DNA methylation of cytosine residues constitutes a prominent epigenetic modification of the chromatin fibre which is locked in a transcriptionally inactive conformation leading to gene silencing. Plant developmental processes, as differentiation and proliferation, are accompanied by chromatin remodeling and epigenetic reprogramming. Despite the increasing knowledge gained on the epigenetic mechanisms controlling plant developmental processes, the knowledge of the DNA methylation regulation during relevant developmental programs in flowering plants, such as gametogenesis or embryogenesis, is very limited. The analysis of global DNA methylation levels has been frequently conducted by high performance capillary electrophoresis, and more recently also by ELISA-based assays, which provided quantitative data of whole organs and tissues. Nevertheless, to investigate the DNA methylation dynamics during plant development in different cell types of the same organ, the analysis of spatial and temporal pattern of nuclear distribution of 5-methyl-deoxy-cytidine (5mdC) constitutes a potent approach. In the present work, immunolocalization of 5mdC on sections and subsequent confocal laser microscopy analysis have been applied for *in situ* cellular analysis of a variety of plant cells, tissues and organs with different characteristics, e.g. hardness, heterogeneity, cell accessibility, tissue compactness, etc. results demonstrated the versatility and feasibility of the approach for different plant samples, and revealed defined DNA methylation nuclear patterns associated with differentiation and proliferation events of various plant cell types and developmental programs. Quantification of 5mdC immunofluorescence intensity by image analysis software also permitted to estimate differences in global DNA methylation levels among different cells types of the same organ during development.

INTRODUCTION

DNA methylation of cytosine residues constitutes a prominent epigenetic modification of the chromatin fibre which is locked in a transcriptionally inactive conformation leading to gene silencing. Generally open chromatin increases the accessibility of the genome to transcription machinery, while closed chromatin represses gene expression by limiting the accessibility (Kouzarides, 2007; Pfluger and Wagner, 2007; Reyes, 2006). Changes in this epigenetic mark, together with histone modifications, result in changes in nucleosome conformation which finally alter DNA accessibility of factors responsible for activation or repression of gene expression. Since chromatin regulation plays a critical role in determining cell fate of totipotent cells, the organization of chromatin domains provides an additional platform for a regulatory level controlling genetic information (Sang et al., 2009).

There are increasing evidences that numerous processes of plant development and differentiation are accompanied by chromatin remodeling and epigenetic reprogramming (Kouzarides, 2007; Tessadori et al., 2007). Epigenetic control plays an essential role in the process of cellular differentiation allowing cells to be reprogrammed in order to generate new differentiation pathways (Costa and Shaw, 2007; Kouzarides, 2007). The architecture of the cell nucleus is highly dynamic and organized in distinct functional domains which modify their organization in response to changes in the nuclear function and gene expression during plant developmental processes (Seguí-Simarro et al., 2006, 2011; Testillano et al., 2000, 2005). However, the relationship between DNA methylation and large-scale organization of nuclear architecture is poorly understood. New evidences showed that changes in DNA methylation accompany the reorganization of the nuclear architecture during plant developmental processes and particularly in cell differentiation, proliferation, and reprogramming (Kumaran et al., 2008; Meijón et al., 2009; Solís et al., 2012).

Research in the past years has revealed exciting findings with regard to epigenetic mechanisms controlling plant developmental processes (Twell, 2011; Zluvova et al., 2001). However, the knowledge of the DNA methylation regulation during relevant developmental programs in flowering plants, such as gametogenesis or embryogenesis, is very limited (Solís et al., 2012; Twell, 2011). Several reports, using

biochemical analysis of whole organs, have described changes in the global methylation levels of DNA with the differentiation of plant reproductive organs (Meijón et al., 2009; Ribeiro et al., 2009; Zhao et al., 2008; Zluvova et al., 2001). Nevertheless, data on the modifications in the nuclear distribution pattern of the methylated DNA *in situ* in relation to the chromatin pattern dynamics is still very scarce. Difficultly in accessing specific cell types inside organs and tissues, like for example the very young embryo or endosperm inside the maternal tissues or the developing microspores inside the anthers, has made biochemical and molecular analysis sometime problematic, as well as the studies at cellular and subcellular levels have been especially difficult. Although partially overcome by the use of *in vitro* systems, *in situ* localization approaches using modern bioimaging technology have became essential tools (Testillano and Rodríguez 2012, Rodríguez-Serrano et al. 2012). The exploitation of fluorescent probes and antibodies has significantly contributed to the analysis of cellular and subcellular events; the challenge of these *in situ* methodologies has been to overcome the limitations associated with the specific features of various plant cells compartments such as cell wall, endocytic compartment, vacuoles, etc.

To investigate the global DNA methylation dynamics during plant development, the analysis of spatial and temporal pattern of nuclear distribution of 5-methyl-deoxy-cytidine (5mdC) constitutes a potent approach, which permitted to distinguish among cell types and processes in the same organ, in comparison with the electrophoretic and ELISA assays used to quantify the percentage of methylated cytidines in genomic DNA. In the present work, immunolocalization of 5mdC and confocal analysis have been applied to several plant cells types and organs with different characteristics for *in situ* cellular analysis on section, *e.g*. hardness, heterogeneity, cell accessibility, tissue compactness, etc; the results demonstrated the versatility and feasibility of the approach for different plant samples, and revealed defined DNA methylation nuclear patterns associated with differentiation and proliferation events of various plant cell types and developmental programs. Quantification of 5mdC immunofluorescence intensity by appropriate confocal image software also permitted to estimate differences in global DNA methylation levels among different cells types of the same organ during development and under different physiological conditions.

MATERIAL AND METHODS

Plant material

Nicotiana tabacum L. plants were grown in a growth chamber (MLR 350H, SANYO) at 25ºC, 80 % humidity and a photoperiod of 16 hours of light. Flower buds and anthers were excised and processed for further analysis. Bulbs of *Allium cepa* L. were germinated in water under standard conditions, and after two days root segments corresponding to the proliferating meristematic zones were selected. Some dried bulbs, not subjected to germination conditions, were used to obtain quiescent root meristems which were excised from the interior of bulbs.

Fixation and processing for immunofluorescence

Root samples were used as plant material which is homogeneous in hardness and easy to section without embedding media. They were processed for cryostat and vibratome sectioning. Anthers were selected as a more heterogeneous plant material in which pollen grains inside the anther cannot be sectioned with cryostat or vibratome. Anthers were processed for embedding in an appropriate acrylic resin. All samples were fixed in 4% paraformaldehyde in phosphate buffered saline (PBS) at 4ºC overnight.

- *Processing for vibratome and cryostat sectioning*

After fixation, root samples were washed in PBS and either, directly sectioned in the vibratome or cryoprotected in sucrose (gradual infiltration in sucrose solutions: 0.1 M for 1 hour, 1 M for 1 hour and 2.3 M for 3 hours, at 4ºC), embedded in OCT compound and frozen on dry ice for sectioning in the cryostat. Thirty-forty micrometers thick vibratome sections were obtained and placed on a drop of water over 3-aminopropyl-triethoxy-silane (APTES)-coated slides, air-dried and stored at -20ºC until use for immunofluorescence (IF). Ten-twenty micrometers thick cryostat sections were collected in glass slides, washed with water to eliminate the OCT and transferred to a water drop over silanized slides; they were finally air-dried and stored at -20ºC until use for IF.

- Processing for low-temperature resin embedding and semithin sectioning

Fixed anthers were washed in PBS and processed for embedding at low temperatures in either Technovit 8100 resin (Kulzer, Germany) or K4M Lowicryl resin (Polysciences). For Technovit 8100, anthers were dehydrated in an acetone series and embedded at 4ºC, as previously described (Solís et al., 2008). For K4M Lowicryl, samples were dehydrated in a methanol series by Progressive Lowering of Temperature (PLT) and finally embedded at -30ºC under UV light in a Leica AFS device, as described previously (Testillano et al., 2000). One-two micrometers semithin sections were obtained from all resin-embedded samples, placed over a drop of water on APTES-coated slides, air-dried and stored at 4ºC until use for immunofluorescence.

5-deoxy-methyl-cytidine immunofluorescence

For vibratome and cryostat sections, permeabilization was required prior to immunofluorescence. The freezing of the sections and storage at -20ºC after their collection, followed by thawing at room temperature constituted the first permeabilization step. After bringing to room temperature, glass slides bearing the sections were first dehydrated in a methanol series (30º, 50º, 70º, 90º, 100º; 5 min each) and rehydrated in a methanol series (90º, 70º, 50º, 30º; 5 min each) and Phosphate Buffered Saline (PBS). They were subsequently subjected to a mild enzymatic digestion of cell walls for additional permeabilization by treatment with 2% (w/v) cellulase in PBS for 1 h. Then, sections were washed three times for 5 min in PBS followed by the immunodetection. Semithin resin sections did not required permeabilization and were subjected directly to the immunodetection, after incubation in PBS for a few minutes. At this step, all section types followed the same protocol of immunofluorescence. Sections were denatured with 2N HCl for 45 min and then blocked with 5% (w/v) Bovine Serum Albumine (BSA) in PBS for 10 min. Sections were then incubated for 1h with the mouse monoclonal anti-5mdC antibody (Eurogentec, Cat. N. BI-MECY-0100, Liege, Belgium) diluted 1:50 in 1% BSA in PBS. After three rinsing steps in PBS, sections were incubated for 45 min in darkness with the secondary antibody, an anti-mouse IgG conjugated to Alexa Fluor 488 (Molecular Probes; Leiden, The Netherlands) diluted 1:25 in 1% BSA. After washing in PBS, nuclei were stained with DAPI (4.6-diamidino-2-phenylindole), washed in sterile water, mounted in Mowiol and examined in a confocal microscope (Leica TCS-SP2-AOBS; Vienna, Austria). Confocal optical

sections were collected either at 0.5 μm or 0.1 μm z-intervals for vibratome/cryostate or resin sections respectively. Images of maximum projections were obtained with software running in conjunction with the confocal microscope (Leica software LCS version 2.5).

Control of immunofluorescence experiments

- *Elimination of the DNA denaturation step.*

A control was performed in all the section types and materials used by performing the whole immunofluorescence protocol and eliminating the DNA denaturation step by avoiding the HCl treatment before the antibody incubation.

- *Immunodepletion of the antibody with 5mdC.*

Pre-blocking of the anti-5mdC antibodies with its corresponding immunogen, the 5mdC (Sigma-Aldrich) was performed by incubating the antibody with and a 5mdC solution (5 μg/μl in water) in a proportion of 1:2, v/v, at 4ºC, overnight. The preblocked antibody solution was used as primary antibodies for immunofluorescence on the sections, following the same protocol and conditions as described above.

Quantification of fluorescence intensity in 5mdC immunolocalization confocal images

For each immunofluorescence microscopy preparation, confocal optical sections were collected at 0.5μm z-intervales, for vibratome and cryostate sections, and at 0.1μm z-intervales for resin sections, with a total of 15 sections. Images of maximum projections were obtained and used for relative fluorescence intensity quantification with software running in conjunction with the confocal microscope (Leica software LCS version 2.5). Fluorescence intensity quantification was performed on random nuclei of each sample, over 30 nuclei were measured per sample, repeating the experiment at least three times. The minimum sample size was determined by the progressive mean technique. *P-values* were calculated using *t-Student* test.

Quantification of global DNA methylation

High Performance Capillary Electrophoresis (HPCE)

To quantify global DNA methylation levels of the three plant cell types studied, microspores, tapetal cells and root meristems, hydrolyzed DNA was prepared as previously described (Solís et al., 2012). Genomic DNA was extracted using a plant genomic DNA extraction kit (DNeasy Plant Mini, Qiagen) according to the manufacturer's instructions. DNA was concentrated and resuspended to a concentration of 1 µg/µl, denatured by heat and cooling rapidly in ice. DNA was hydrolized by treatments with: a) 10 mM $ZnSO_4$ and 0.5 µl of nuclease P1 (Sigma; 200 U/ml) for 16 h at 37 °C, and b) 0.25 µl alkaline phosphatase (Sigma; 50 U/ml) for 2 h at 37°C. Hydrolyzed solutions were centrifuged for 20 min at 15,000g and analyzed by HPCE using capillary electrophoresis instruments CIA (Waters Chromatography) and PACE 2050 (Beckman), using the method and conditions previously described (Solís et al., 2012). Quantification of the relative DNA methylation level of each sample was calculated as the percentage of 5-methyl-deoxy-cytidines (5mdC) peak of total deoxy-cytidines (dC+5mdC) peaks. Three biological and two analytical replicates per sample were taken. *P-values* were calculated using *t-Student* test.

5mdC ELISA-based immunoassay

To compare relative levels of global DNA methylation between root meristems in proliferating and quiescent conditions, a MethylFlash Methylated DNA Quantification Kit (Colorimetric) (Epigentek, NY, USA) was used according to the manufacturer's instruction using 100 ng of genomic DNA for each sample (Li and Liu, 2011). Total DNA was extracted using a plant genomic DNA extraction kit (DNeasy Plant Mini, Qiagen) according to the manufacturer's instructions. The purified DNA was added to an ELISA plate where the methylated fraction of DNA was quantified using 5-deoxy-methyl-cytosine specific antibodies. The amount of methylated DNA was proportional to the OD (optical density) intensity measured in an ELISA plate reader at 450 nm. After subtracting negative control readings from the readings for the sample and the standard, the value of 5-methyl-deoxy-cytosine for each sample was calculated as a ratio of sample OD relative to the standard OD. Results were expressed as the

percentage of methylated deoxycytosines of total DNA. The assay was performed in triplicate. *P-values* were calculated using *t-Student* test.

RESULTS AND DISCUSSION

Fluorescent *in situ* localization of 5mdC on sections, a reliable approach to analyze DNA methylation pattern dynamics in different plant cell types

To evaluate the feasibility of the 5mdC immunofluorescence for plant materials, plant samples with different characteristics for *in situ* cellular analysis on section were used: root meristems and anthers. The root meristem was chosen as a sample with low/mild hardness and relatively homogeneous structure; therefore, it could be sectioned without embedding media by either the vibratome or the cryostate, providing thick sections with good structural preservation. The anther was an organ more heterogeneous, composed by very different cell types with different wall hardness and vacuoles; moreover, the anthers contained microspores and pollen grains inside the pollen sac which would be lost in non-embedded sections; therefore the anthers were processed and embedded in acrylic resins at low temperature, to maintain their structural integrity and to preserve their antigenic properties as much as possible. The resins of choice were Technovit 8100 and Lowicryl K4M.

The protocols have been designed to obtain reliable and successful results, taken into account the particular properties of each cell type and tissue studied. They were described in details in the Material and Methods section and involved several permeabilization steps for vibratome and cryostate sections, including freezing-thawing, dehydration-rehydration and mild cell wall enzymatic digestion. After permeabilization, vibratome and cryostate sections were treated with the same protocol than resin sections. Denaturation of the DNA in sections with HCl was essential to expose the 5mdC antigen to the antibodies. Further steps included the blocking and the incubations with the first (anti-5mdC) and secondary (fluorochrome-Alexa-conjugated) antibodies.

The microscopical analysis of the immunofluorescence preparations was performed in a confocal laser scanning microscope (CLSM) which permitted to obtain optical sections and avoided the out-of-focus fluorescence of the thick (30-50 μm) vibratome-cryostat sections. 1-2 μm semithin resin sections could be analyzed by both CLSM and epifluorescence microscopes, even though the CLSM provided fluorescent images of higher resolution and quality. The results obtained were similar in both

vibratome-cryostat and resin sections (Figs. 1a-e, 4a-f). They exhibited intense immunofluorescence signals on defined regions of the nuclei, which were clearly identified by DAPI staining, in all the plant samples analyzed, showing different nuclear distribution patterns depending on the cell type, plant species and developmental stage (Figs. 1a-e, 4a-f); no fluorescence signal was observed in other cellular compartments which appeared dark.

Controls performed by eliminating the DNA denaturation by HCl showed a complete absence of signal (Fig. 2a-c) indicating that the antibody did not cross-react with double-stranded DNA or other nuclear antigens. Immunodepletion experiments were carried out by pre-blocking the antibody with the antigen (5mdC) *in vitro* and using this pre-blocked antibody for immunofluorescence assays. The analysis showed negative results (Fig. 2d-f) indicating that the antibody only recognized the 5mdC as antigen and did not cross-react with other antigens, since it was completely blocked *in vitro* with the 5mdC, these results of the immunodepletion experiments additionally validated the specificity of the immunofluorescence signal obtained. In some cases, the special microspore wall, the exine, exhibited unspecific autofluorescence (Fig. 2e) which, in section, did not interfere with the specific fluorescence signal of the target cell compartments (nucleus).

Immunocytochemical approaches on plant biology research are often constrained by their application to either tissues and organs or suspension culture cells, which oblige to section the samples before the immunoreactions or to perform them *in toto* after intense permeabilization treatments. Frequently, antibodies have shown very low or no reactivity *in situ* to their targets in plant subcellular compartments due to their limited penetration through thick sections (vibratome and cryostat thick sections), or their low sensibility to react with the antigens exposed on the surface of resin sections. The immunofluorescence approach presented here constitutes a feasible and reliable method for the *in situ* analysis of DNA methylation nuclear patterns in a wide range of plant systems, since it can be successfully applied to samples treated by different processing methods, e.g. resin-embedded semithin sections, vibratome and cryostat thick sections. The approach has therefore a high potential for *in situ* epigenetic studies during plant development since it can be easily performed to very different plant tissues and organs, pollen grains and isolated cells.

Investigations of chromosome organization and arrangement in the nucleus have been conducted since the beginning of cell biology research. There are increasing evidences that numerous processes of development and differentiation in both plants and animals are accompanied by chromatin remodelling (Kouzarides, 2007). Epigenetic modifications, like DNA methylation and histone modifications have been revealed as hallmarks that define the functional status of chromatin domains and confer the flexibility of transcriptional regulation necessary for plant development and adaptative responses to the environment (Grant-Downton and Dickinson, 2005; Solís et al., 2012; Vaillant and Paszkowski, 2007). Histone modification and DNA methylation patterns are expected to affect chromosome organization, although data on this subject are still scarce, especially in plant systems. The DNA methylation nuclear patterns of different plant cell types and their dynamics in relation to chromatin organization during proliferation and differentiation processes can be easily characterized by the approach presented here, based on the versatility of the immunolocalization protocol used and the good resolution and quality provided by the CLSM analysis; the information raised will give new insights into the mechanisms regulating epigenetic patterns and chromatin remodelling during plant development and adaptation.

Different nuclear patterns of DNA methylation are revealed by 5mdC immunofluorescence in microspores and tapetal somatic cells of the anther

The 5mdC immunofluorescence signal showed different nuclear distribution patterns depending on the cell type, plant species and developmental stage. In tobacco anthers, the developing microspores at the stage of vacuolated microspores, showed rounded nuclei and a large cytoplasmic vacuole which pushed the nucleus out of the middle (Fig. 1c). At this particular developmental stage the microspores have been reported highly active in transcription (Testillano et al., 2000, 2005). The nuclei of the vacuolated microspores exhibited faint 5mdC fluorescence throughout the whole nucleus, while the nucleolus appeared dark; the distribution pattern followed a thin network with a few spots (Figs. 1b, c) which corresponded to the low condensed chromatin state of the microspores at this stage of development (Testillano et al., 2005).

The tapetal cells are the nutritive tissue of the microsporocytes in the anther, they differentiate in parallel with microspore development until the microspore vacuolation and the first pollen mitosis when the tapetum initiates a programmed cell death program. They are binucleate differentiated polyploid cells which play an important nursing role during early pollen development (Hesse et al., 1993); they are located in the inner face of the anther wall (Fig. 1c). The nuclei of the tapetal cells displayed an intense 5mdC immunofluorescence, with numerous and larger spots forming a thick network in the whole area of the nucleus (Figs. 1b, c, e), as corresponded to the relatively high degree of chromatin condensation of these cells (Testillano et al., 1993). The quantification of the immunofluorescence intensity per area in the two cell types (Fig. 1f) clearly supported the qualitative results observed. The relative fluorescence intensity of tapetal nuclei was significantly higher (107.80± 6.49) than the signal intensity of the microspores (52.30±7.24) (Fig. 1f).

The quantification of global DNA methylation levels by high performance capillary electrophoresis (HPCE) provided information on the percentage of methylated deoxy-cytosines (5mdC) of the total deoxy-cytosines (5mdC+dC). HPCE has been performed on tapetal cells and isolated microspores which were extracted from the anthers. The analysis showed higher levels of DNA methylation in the tapetum (7.76% ± 0.93 mdC of total dC) than in the vacuolated microspores (3.42% ± 0.62 mdC of total dC) (Fig. 3). This data was in agreement with the different immunofluorescence signals observed between the two cell types (Figs. 1a-e) and correlated with the quantification of the immunofluorescence intensities (Fig. 1f), giving additional support to the specificity and sensitivity of the *in situ* immunolocalization assay. In contrast with the HPCE assay, the immunofluorescence approach presented not only provided with a reliable estimation of differences in global methylation levels, but also revealed the *in situ* pattern of distribution of methylated DNA in relation to the chromatin condensation pattern.

Chromosome organization has been shown to change during plant development and in response to the environmental conditions. Dynamic changes between chromatin states that facilitate or inhibit DNA transcription are relevant in the transcriptional regulation during pollen development (Testillano et al., 2005, Seguí-Simarro et al., 2011). Several reports have revealed that heterochromatin increases during cell

differentiation and organ maturation, while it decreases during cell proliferation and de-differentiation (Solís et al., 2012; Tessadori et al., 2007; Testillano et al., 2000, 2005). Chromocenters, the heterochromatin masses of the centromere regions of chromosomes, become smaller in leaves prior to the transition to reproductive development and recover to their former size after the elongation of the floral stem (Tessadori et al., 2007; Tiang et al., 2012). Changes in the ploidy level generated by endoreduplication have been shown to affect chromosome arrangement in *Arabidopsis* (Berr and Schubert, 2007). On the other hand, several studies have described an increase on the global methylation levels of DNA with the differentiation of plant reproductive organs (Meijón et al., 2009; Ribeiro et al., 2009; Zhao et al., 2008; Zluvova et al., 2001), but the nuclear distribution pattern of the methylated DNA has not been analyzed in those systems.

The results presented here, showed differences in the distribution pattern of the 5mdC in two plant cell types of the anther, the microspore and the tapetal cell in relation to their different chromatin condensation pattern. The microspore is transcriptionally very active at the particular developmental stage of vacuolated microspore (Testillano et al., 2005), showing a decondensed chromatin pattern with scarce and small heterochromatin masses (Testillano et al., 2005), whereas the tapetal cells are in a highly differentiated state with numerous heterochromatin masses (Testillano et al., 1993). The differences in the 5mdC distribution pattern were associated with defined heterochromatin organizations, which subsequently reflected differences in the developmental program and the transcriptional activity of each cell type, microspores and tapetal cells. High 5mdC immunofluorescence signal was associated with high heterochromatization (chromatin condensation) during late differentiation in the tapetal nuclei, while lower signal accompanied the vacuolated microspore which exhibited a more decondensed chromatin organization and has been reported with a high transcriptional activity at this stage of development (Testillano et al., 2005).

Cycling and quiescent root meristematic cells showed different nuclear patterns of DNA methylation revealed by 5mdC immunofluorescence

The root meristem constitutes a good model of proliferating cells for the analysis of DNA methylation dynamics. In germinating conditions, the root meristem was formed by lines of cycling cells showing typical interphase nuclei and mitotic chromosomes

(Figs. 4a-f). Proliferating root meristems were also analyzed by HPCE to quantify the percentage of DNA methylation; the results showed a low global methylation level (1.97% ± 0.35 mdC of total dC) of the proliferating root cells in comparison with the differentiating microspores and tapetal cells (Fig. 3). This result suggested a relationship between low DNA methylation degree and plant cells in active proliferation. On the contrary, higher methylation levels were associated with plant cells in differentiation, like microspores and tapetal cells (Fig. 3).

Confocal microscopy analysis of proliferating root tips showed 5mdC immunofluorescence signals of medium intensity that appeared decorating the nuclei of meristematic cells with different distribution patterns, whereas the nuclei of the root cap cells exhibited more intense fluorescence signals (Figs. 4a, b, and insets) corresponding with their higher degree of chromatin condensation. In cycling interphasic nuclei, the 5mdC fluorescence exhibited different intensities and distribution patterns (Figs. 4c, d); probably corresponding to nuclei at different interphase periods of the cell cycle presenting different chromatin condensation states. Nuclei of cycling meristematic cells showed the 5mdC signal as a thin reticulum covering the whole nucleus area, with different intensities and thickness threads on individual nuclei (Figs. 4c, d), the nucleoli did not show fluorescence in any case, appearing as dark rounded regions in both DAPI and 5mdC micrographs. Mitotic chromosomes exhibited an intense 5mdC immunofluorescence along the chromosome arms (Figs. 4c, d), as corresponds to their high condensation. In some cases more intense signals were found at the chromosomal periphery, close to the region where nucleolar RNPs are relocated during metaphase and anaphase, as described in plant cells by silver impregnation methods (Medina et al., 1986; Risueño and Medina, 1986), and in animal cells (Hernández-Verdún and Gautier, 1994). Recently, regions of highly methylated DNA have been identified along chromosomes of *Brachypodium distachyon* in squash preparations, relating them to the condensation degree and structure of the chromosomes (Borowska et al., 2011). The method presented here could help to analyze the methylation patterns of chromosomes during different mitotic phases which can be clearly identified on sections of proliferating meristems, rather than on squash preparations.

The quiescent root meristems were obtained from onion bulbs in non-germinating conditions; therefore, they contained meristematic cells that were not active

in proliferation. The pattern of 5mdC immunofluorescence obtained in quiescent root meristematic cells was different than that of cycling cells. The signal appeared very intense in the nucleus (Figs. 4e, f), however the nucleolus did not show any labelling. This homogeneous and high 5mdC signal revealed a pattern of DNA methylation in quiescent nuclei consistent with the inactive state of the cells and the condensed chromatin organization reported for quiescent root cells (Risueño and Moreno-Díaz de la Espina et al., 1979). The immunofluorescence intensity was quantified in the interphasic nuclei of proliferating and quiescent roots. The results showed that quiescent root nuclei exhibited relative fluorescence intensity significantly higher (68.40±9.15) than the nuclei of proliferating roots (42.10±3.73) (Fig. 4g), the quantification of the immunofluorescence intensity supporting clearly the differences observed in the confocal images (Fig. 4g).

To compare the relative amounts of methylated DNA between proliferating and quiescent root meristems, an ELISA-based assay (Eurogentek, NY, USA) was performed (Li and Liu 2011). The results showed significant differences among roots under the two different physiological conditions (Fig. 4h), the quiescent roots showing higher levels of DNA methylation (0.83% ± 0.03 mdC of total DNA) than the proliferating ones (0.63% ± 0.04 mdC of total DNA). This data was in agreement with the different immunofluorescence signals obtained in the two types of root meristems with very different activity states (Figs. 4c-f), as well as with the quantification of their fluorescence intensities (Fig. 4g); the higher transcriptional activity of proliferating roots being associated with the lower DNA methylation level obtained, while the lower activity of quiescent roots was accompanied by a higher percentage of methylated DNA (Fig. 4h). Taken together, these results indicated that the 5mdC *in situ* localization presented here constitutes a convenient approach to characterize changes in DNA methylation nuclear patterns and to estimate differences in global methylation levels, not only among different cells types of the same organ during development, but also in a particular cell type under different physiological conditions.

During interphase, chromosomes assume a largely decondensed state. However, chromatin is still non-randomly arranged within the nuclear space. Each chromosome occupies a limited, exclusive nuclear subdomain, known as a chromosome territory

(reviewed in Tiang et al., 2012). Even though there has been a growing interest in understanding how chromosome and chromatin arrangement in interphase nuclei affect gene activity, effects of chromatin organization on gene expression are still poorly understood in plants. The analysis the DNA methylation pattern dynamics as epigenetic mark of the chromatin functional state in relation to the nuclear architecture will help to understand how interphase chromosome arrangement affects gene expression during plant growth and development in plants, and in response to specific environmental conditions. The results of the present work revealed a change in the DNA methylation nuclear pattern of meristematic root cells caused by different external conditions: non-germinating conditions which keep the meristem in a quiescent state, and germinating agents inducing meristem proliferation and root growth. The data suggested that DNA methylation nuclear pattern dynamics accompany the modifications of chromatin condensation associated with the activation of proliferation, which can be driven by external conditions and inner signals inducing specific growth processes.

ACKNOWLEDGEMENTS

Thanks are due to Prof. María-Jesús Cañal (BOS Department, Oviedo University, Spain) and Prof. Alejandro Cifuentes (CIAL, CSIC, Madrid, Spain) for their help with the HPCE analysis, and to Ms. Alicia Rodríguez-Huete for her skillful technical work. Work supported by projects granted by the Spanish Ministry of Science and Innovation (MICINN), BFU2011-23752, BFU2008-00203 and AGL2008-04255, and CSIC, PIE 201020E038.

REFERENCES

Berr A and Schubert I (2007) Interphase chromosome arrangement in *Arabidopsis thaliana* is similar in differentiated and meristematic tissues and shows a transient mirror symmetry after nuclear division. Genetics 176:853-863.

Borowska N, Idziak D and Hasterok R (2011) DNA methylation patterns of *Brachypodium distachyon* chromosomes and their alteration by 5-azacytidine treatment. Chromosome Research 19:955-967.

Costa S and Shaw P (2007) 'Open minded' cells: how cells can change fate. Trends in Cell Biology 17:101-106.

Grant-Downton RT and Dickinson HG (2005) Epigenetics and its implications for plant biology. 1. The epigenetic network in plants. Annals of Botany 96:1143-1164.

Hernández-Verdún D and Gautier T (1994) The chromosome periphery during mitosis. Bioessays 16:179-185.

Hesse M, Pacini E and Willemse M (1993) The tapetum. Cytology, Function, Biochemistry and Evolution. Springer-Verlag Wien New York.

Kouzarides T (2007) Chromatin modifications and their function. Cell 128:693-705.

Kumaran RI, Thakar R and Spector DL (2008) Chromatin dynamics and gene positioning. Cell 132:929-934

Li W and Liu M (2011) Distribution of 5-hydroxymethylcytosine in different human tissues. Journal of Nucleic Acids, Volume 2011, Article ID 870726, doi:10.4061/2011/870726

Medina FJ, Solanilla EL, Sanchez-Pina MA, Fernández-Gómez ME and Risueño MC (1986) Cytological approach to the nucleolar functions detected by silver staining. Chromosoma 94:259-266.

Meijón M, Valledor L, Santamaría E, Testillano PS, Risueño MC, Rodríguez R, Feito I and Cañal MJ (2009) Epigenetic characterization of the vegetative and floral stages of azalea buds: Dynamics of DNA methylation and histone H4 acetylation. Journal of Plant Physiology 166:1624-1636.

Pfluger J and Wagner D (2007) Histone modifications and dynamic regulation of genome accessibility in plants. Current Opinion in Plant Biology 10:645-652.

Reyes JC (2006) Chromatin modifiers that control plant development. Current Opinion in Plant Biology 9:21-27.

Ribeiro T, Viegas W and Morais-Cecilio L (2009) Epigenetic marks in the mature pollen of *Quercus suber* L. (*Fagaceae*). Sexual Plant Reproduction 22:1-7.

Risueño MC and Medina FJ (1986) The nucleolar structure in plant cells. Cell Biology Reviews 7:1-213.

Risueño MC and Moreno-Díaz-de-la-Espina S (1979) Ultratructural and cytochemical study of the nucleus of the dormant root meristematic cells. Journal of Submicroscopical Cytology 11:85-98.

Rodríguez-Serrano M, Barany I, Prem D, Coronado MJ, Risueño MC, Testillano PS. (2012) NO, ROS and cell death associated with caspase-like activity increase in stress-induced microspore embryogenesis of barley. Journal of Experimental Botany, 63, 2007-2024.

Sang Y, Wu MF and Wagner D (2009) The stem cell--chromatin connection. Seminars in Cell and Developmental Biology 20:1143-1148.

Seguí-Simarro JM, Bárány I, Suárez R, Fadón B, Testillano PS and Risueño MC (2006) Nuclear bodies domain changes with microspore reprogramming to embryogenesis. European Journal of Histochemistry 50:35-44.

Seguí-Simarro JM, Corral-Martínez P, Corredor E, Raska I, Testillano PS and Risueño MC (2011) A change of developmental program induces the remodelling of the interchromatin domain during microspore embryogenesis in *Brassica napus L.* Journal of Plant Physiology 168:746-757.

Solís MT, Pintos B, Prado MJ, Bueno MA, Raska I, Risueño MC and Testillano PS (2008) Early markers of *in vitro* microspore reprogramming to embryogenesis in olive (*Olea europaea* L.). Plant Science 174:597-605.

Solís MT, Rodríguez-Serrano M, Meijón M, Cañal MJ, Cifuentes A, Risueño MC and Testillano PS (2012) DNA methylation dynamics and *MET1a-like* gene expression changes during stress-induced pollen reprogramming to embryogenesis. Journal of Experimental Botany, DOI: 10.1093/jxb/ers298.

Tessadori F, Schulkes RK, van Driel R and Fransz P (2007) Light-regulated large-scale reorganization of chromatin during the floral transition in *Arabidopsis*. Plant Journal 50:848-857.

Testillano PS, González-Melendi P, Fadón B, Sánchez-Pina MA, Olmedilla A, Risueño MC (1993) Immunolocalization of nuclear antigens and ultrastructural cytochemistry on tapetal cells. Plant Systematic and Evolution [Suppl. 7]:49-58.

Testillano PS, Coronado MJ, Seguí-Simarro JM, Domenech J, González-Melendi P, Raska I and Risueño MC (2000) Defined nuclear changes accompany the reprogramming of the microspore to embryogenesis. Journal of Structural Biology 129:223-232.

Testillano PS, González-Melendi P, Coronado MJ, Seguí-Simarro JM, Moreno-Risueño MA and Risueño MC (2005) Differentiating plant cells switched to proliferation remodel the functional organization of nuclear domains. Cytogenetics and Genome Research 109:166-174.

Testillano PS and Rodríguez MD (2012) Cell biology of plant development and adaptation, in Hot topics in Cell Biology, Becerra J, Santos-Ruíz L (eds). Biohealthcare Publishing Limited, Oxford, UK. pp 61-62.

Tiang CL, He Y and Pawlowski WP (2012) Chromosome organization and dynamics during interphase, mitosis, and meiosis in plants. Plant Physiology 158:26-34.

Twell D (2011) Male gametogenesis and germline specification in flowering plants. Sexual Plant Reproduction 24:149-160.

Vaillant I and Paszkowski J (2007) Role of histone and DNA methylation in gene regulation. Current Opinion in Plant Biology 10:528-533.

Zhao XY, Su YH, Cheng ZJ and Zhang XS (2008) Cell fate switch during *in vitro* plant organogenesis. Journal of Integrative Plant Biology 50:816-824.

Zluvova J, Janousek B and Vyskot B (2001) Immunohistochemical study of DNA methylation dynamics during plant development. Journal of Experimental Botany 52:2265-2273.

FIGURE LEGENDS

Figure 1: 5mdC immunofluorescence in microspores and tapetal cells of tobacco anthers. a-e: Confocal images of 5mdC immunofluorescence on 1 µm-semithin sections of Technovit. a-c: Same section of an anther showing microspores (Mic) and tapetum (Tap): (a) DAPI staining, (b) 5mdC immunofluorescence and (c) differential interference contrast (DIC) and 5mdC immunofluorescence merged image. d-e: Details at higher magnification of 5mdC immunofluorescence on microspore (d) and tapetal (e) nuclei. f: Quantification of 5mdC immunofluorescence signal intensity. Histogram representing the mean values of relative fluorescence intensity in arbitrary units of microspores (first column) and tapetal nuclei (second column) of anthers, as measured by confocal image analysis software on maximum projection images. Numbers in columns indicate mean values. Different letters indicate significant differences at $P < 0.001$. PS: Pollen sac. Bars: a, b, c: 30 µm; d, e: 10 µm.

Figure 2: Controls of 5mdC immunofluorescence. Confocal images of 1 µm-semithin Technovit sections of tobacco anthers. a-c: Control avoiding the DNA denaturation by HCl, d-e: Immunodeplection of the antibody by *in vitro* pre-blocking with 5mdC. (a, d) DAPI staining , (b, e) 5mdC immunofluorescence and (c, f) DIC images. Tap: tapetal cells, Mic: microspores, AW: anther wall, PS: pollen sac. Bars: 50 µm.

Figure 3: Quantification of global DNA methylation by HPCE in different plant cells. Histogram representing the values of 5mdC percentage of total dC in tapetal cells (first column), vacuolated microspores (second column) and proliferating root meristems (third column). Numbers in columns indicate mean values. Different letters indicate significant differences at $P < 0.001$.

Figure 4: 5mdC immunofluorescence and quantification of global DNA methylation in proliferating and quiescent root meristematic cells. a-f: Confocal images of 5mdC immunofluorescence on 40 µm-vibratome sections. a-b: Same section of a proliferating root tip showing the root cap (Cap) and the meristematic (Me) cells after DAPI staining (a) and 5mdC immunofluorescence (b); insets show root cap cells at higher magnification. c-d: Details of the cycling cells of the meristem at higher

magnification showing mitotic chromosomes and interphasic nuclei after DAPI staining (c) and 5mdC immunofluorescence (d). e-f: Quiescent meristematic root cells after DAPI staining (e) and 5mdC immunofluorescence (f). g: Quantification of 5mdC immunofluorescence signal intensity. Histogram representing the mean values of relative fluorescence intensity in arbitrary units of quiescent (first column) and proliferating (second column) root meristematic nuclei, as measured by confocal image analysis software on maximum projection images. h: Quantification of global DNA methylation by ELISA-based immunoassay. Histogram representing the values of 5mdC percentage of total DNA in quiescent (first column) and proliferating (second column) onion root meristems. Numbers in columns indicate mean values. Different letters indicate significant differences at $P < 0.001$. Bars: a, b: 150 μm; insets: 45 μm; c-f: 20 μm.

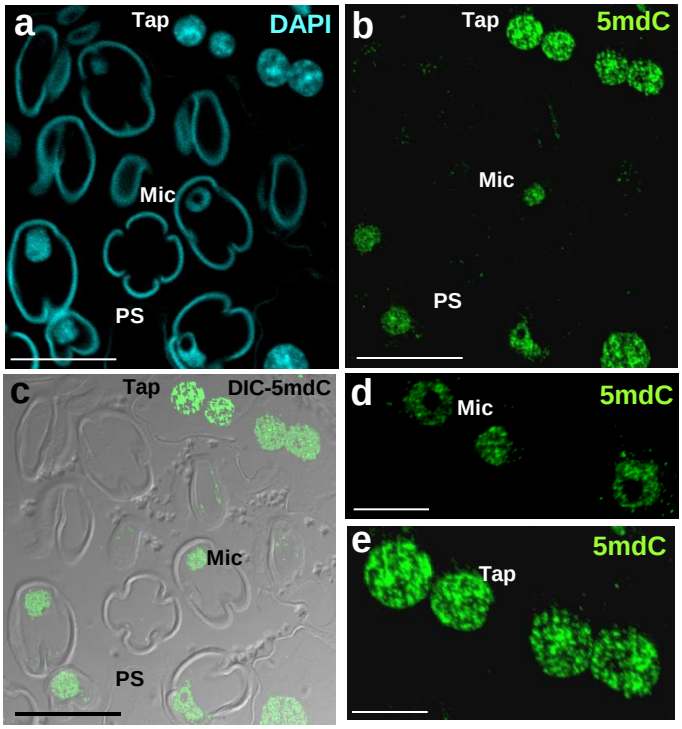
a
Tap
DAPI
Mic
PS
b
Tap
5mdC
Mic
PS
c
Tap
DIC-5mdC
Mic
PS
d
Mic
5mdC
e
5mdC
Tap

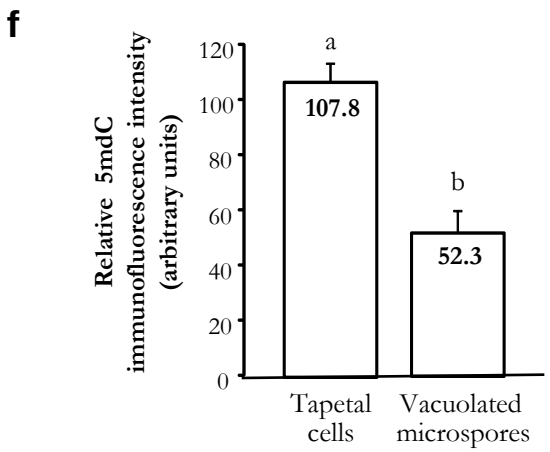
f
Relative 5mdC immunofluorescence intensity (arbitrary units)
120
100
80
60
40
20
0
a
107.8
b
52.3
Tapetal cells
Vacuolated microspores

Figure 1

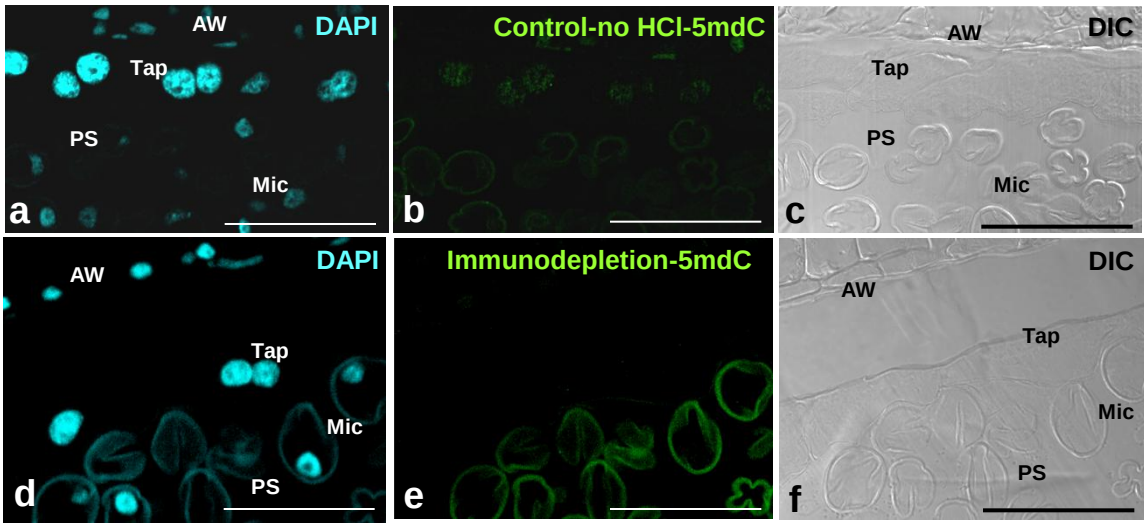
AW
DAPI
Tap
PS
Mic
a
Control-no HCl-5mdC
b
AW
DIC
Tap
PS
Mic
c
AW
DAPI
Tap
Mic
PS
d
Immunodepletion-5mdC
e
DIC
AW
Tap
Mic
PS
f

Figure 2

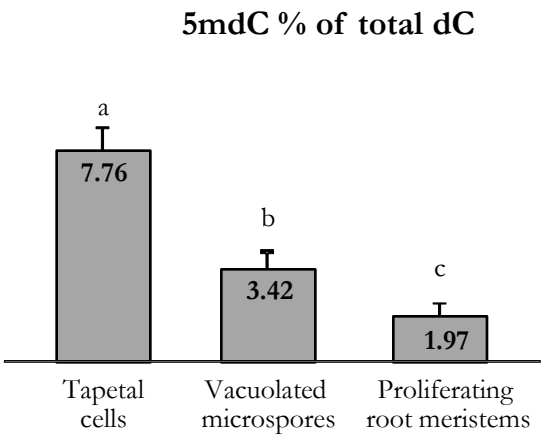
5mdC % of total dC
a
7.76
b
3.42
c
1.97
Tapetal cells
Vacuolated microspores
Proliferating root meristems

Figure 3

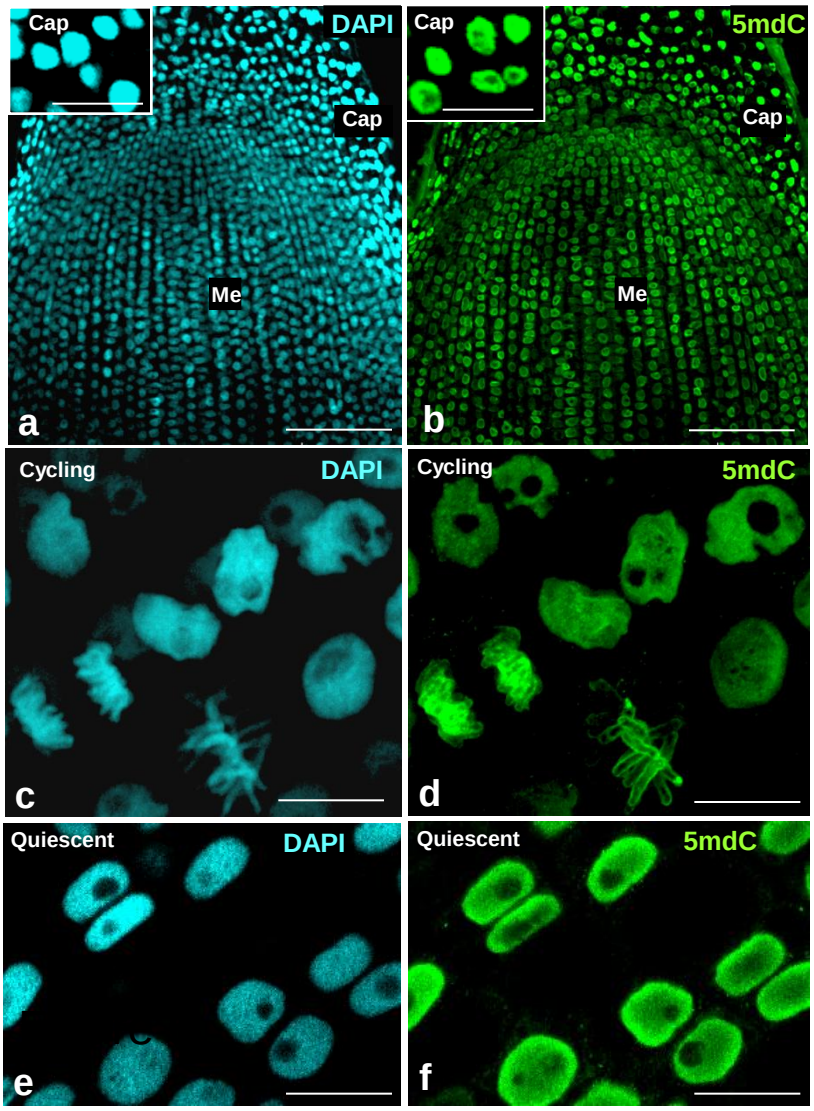
Cap
DAPI
Cap
Me
a
Cap
5mdC
Cap
Me
b
Cycling
DAPI
c
Cycling
5mdC
d
Quiescent
DAPI
e
Quiescent
5mdC
f

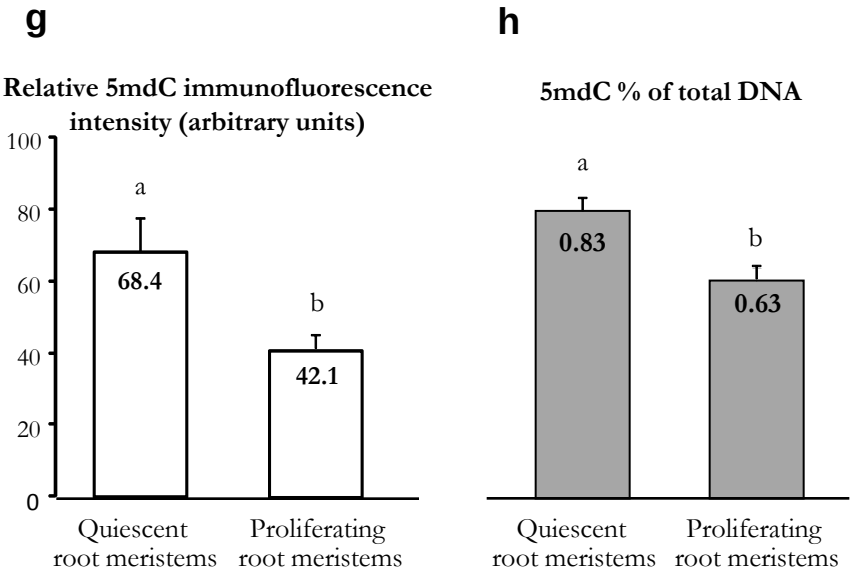
g
Relative 5mdC immunofluorescence intensity (arbitrary units)
100
80
60
40
20
0
a
68.4
b
42.1
Quiescent root meristems
Proliferating root meristems
h
5mdC % of total DNA
a
0.83
b
0.63
Quiescent root meristems
Proliferating root meristems

Figure 4